Structure of Restacked and Pillared WS_2: An X-ray Absorption Study

Eric Prouzet,*,† Joy Heising,‡ and Mercouri G. Kanatzidis*,‡

Institut Européen des Membranes, (CNRS UMR 5635), CNRS, 1919 Route de Mende, F-34293 Montpellier Cedex 5, France, and Department of Chemistry and Center for Fundamental Materials Research, Michigan State University, East Lansing, Michigan 48824

Received April 10, 2002. Revised Manuscript Received October 8, 2002

Exfoliated and restacked tungsten disulfide were characterized by X-ray absorption at the sulfur K edge and tungsten L_3 edge. The local organization around W atoms was probed by EXAFS, by applying a nonGaussian distance distribution model in order to take into account the high disorder in the structure. On the basis of previous structural determinations performed by electron microdiffraction and pair-distribution functions deduced from neutron diffraction, a structural model was tested by comparing the theoretical expected EXAFS signal deduced from this model to the experimental signal. All results converge to prove that upon exfoliation and restacking the WS_2 structure evolves toward a clusterization that gives zigzag chains. Moreover, the local shift of the W atoms is in tandem with a periodic shift of the S atoms along the stacking axis, which causes the layer to deviate from full planarity. Further pillaring with various metal clusters does not affect this structural evolution.

Introduction

Materials with open or accessible frameworks are important in many fields of chemistry, for example, for use in catalytic processes that require large reactive surfaces. Layered transition metal sulfides such as WS_2 or MoS_2 have been shown to be efficient hydrodesulfurization (HDS) catalysts.[1,2] For catalytic applications these materials are prepared as small crystallites deposited on porous supports that provide the expected exchange area. Even in this case, most of the inter-slab surface of these materials cannot be reached by reactants. Moreover, the actual mechanism implied during the catalytic process is not yet fully understood. It was shown that this surface can be made accessible to reactions once the layers have been pillared by chalcogenide clusters of the general formula $Co_6Q_8(PR_3)_6$ (Q = S, Se, Te; and R = Et, Ph).[3] Pillaring was achieved by the addition of $Co_6Q_8(PR_3)_6$ solutions in CH_2Cl_2 to exfoliated suspensions of $LiMoS_2$. This process also applies to WS_2 and extends to other chalcogenide clusters of the type $M_XQ_Y(PR_3)_6$ with M = Co, Fe, Ni; Q = S, Se, Te; and R = Et, Bu, Ph. Effective HDS activity was verified with some of these materials.[4]

Exfoliated MoS_2 and WS_2 are capable of rich intercalation chemistry, but their poorly ordered structures make them good candidates for X-ray absorption spectroscopy (XAS) studies.[5] Joensen et al.[6] first pointed out by EXAFS the huge structural modification in the exfoliated single layers of MoS_2 with a considerable shortening of the Mo−Mo distance, from 3.17 Å in the pristine material to 2.8 Å in the exfoliated one. However, they did not succeed in explaining this phenomenon. Guay et al.[7] also studied restacked and tetrachloroethylene intercalated MoS_2 thin films at both the sulfur and molybdenum edges, but they could not observe any obvious modification in their samples. Zubavichus et al.[8] studied the local structure of MoS_2 intercalated with $M(OH_2)$ (M = Mn, Co, and Ni). They also did not report any drastic change of the local structure (except for the Ni-intercalated samples where a 2.77 Å Mo−Mo distance was in agreement with Joensen's study), but their samples had been stored in air for two months before data collection. They assigned it to the metastability of an octahedral phase obtained by exfoliation,[9] which reverts to the trigonal prismatic 2H pristine phase. Shortly after, Dungey, Curtis and Penner-Hahn reported on the intercalation in MoS_2 by Co and Fe complexes, through an exfoliation/flocculation process.[10] The study at the Mo K edge led to an unexpectedly complex radial distribution compared to previously reported works. They proposed a structural model in which the distorted structure is partially maintained

* Authors to whom correspondence should be addressed. E-mail: prouzet@iemm.univ-montp2.fr, or kanatzi1@pilot.msu.edu.
† Institut Européen des Membranes.
‡ Michigan State University.

(1) Topsøe, H.; Clausen, B. S. *Catal. Rev. −Sci. Eng.* **1984**, *26*, 395.
(2) Chianelli, R. R. *Catal. Rev. −Sci. Eng.* **1984**, *26*, 361.
(3) Bissessur, R.; Heising, J.; Hirpo, W.; Kanatzidis, M. G. *Chem. Mater.* **1996**, *8*, 318.
(4) Brenner, J.; Marshall, C. L.; Ellis, L.; Tomczyk, N.; Heising, J.; Kanatzidis, M. G. *Chem. Mater.* **1998**, *10*, 1244.
(5) Divigalpitiya, W. M. R.; Frindt, R. F.; Morrison, S. R. *Science* **1989**, *246*, 369.
(6) Joensen, P.; Crozier, E. D.; Alberding, N.; Frindt, R. F. *J. Phys. C: Solid State Phys.* **1987**, *20*, 4043.
(7) Guay, D.; Divigalpitiya, W. M. R.; Bélanger, D.; Feng, X. H. *Chem. Mater.* **1994**, *6*, 614.
(8) Zubavichus, Y. V.; Slovokhotov, Y. L.; Schilling, P. J.; Tittsworth, R. C.; Golub, A. S.; Protzenko, G. A.; Novikov, Y. N. *Inorg. Chim. Acta* **1998**, *280*, 211.
(9) Py, M. A.; Haering, R. R. *Can. J. Phys.* **1983**, *61*, 76.
(10) Dungey, K. E.; Curtis, M. D.; Penner-Hahn, J. E. *Chem. Mater.* **1998**, *10*, 2152.

10.1021/cm021186z CCC: $25.00
Published on Web 12/18/2002

upon exfoliation and restacking, with Mo atoms shifted from their initial position to form trigonal clusters. Unfortunately, they did not specify the time between sample preparation and experiments. This point appears to be very important because Ouvrard et al. confirmed by studying both fresh and older samples that restacked MoS_2 is metastable and that it recovers its pristine structure quickly.[11] We also have experimental evidence that restacked WS_2 is much more stable on standing than restacked MoS_2.[12] Hence, it appears that conclusions of previous studies, especially those reporting on MoS_2, must be carefully considered. Ouvrard et al. pointed out also that describing the phase transition such as a *2H*- to *1T*-MoS_2 transition as stated previously[9,10] was too simplistic. For these authors, the shift of the Mo atoms implies that the new sites cannot be described anymore as either trigonal prismatic or octahedral. Unlike Dungey et al., they claimed that molybdenum atoms should shift in order to build tetrameric diamond-shaped clusters. They showed that this model could explain the changes observed by EXAFS. The Mo cluster formation in $LiMoS_2$ was also sustained by FLAPW calculations.[13]

Different hypotheses were thus proposed for the structural evolution of both molybdenum and tungsten disulfides upon intercalation/exfoliation and restacking.

In the course of the preparation of pillared layered metal sulfides,[3,4,14] we initiated a study of the structure of restacked MoS_2 and WS_2 by X-ray diffraction[15] and electron diffraction.[16] This latter study found that the structure of restacked WS_2 and MoS_2 resembles the one of WTe_2.[17] The key feature in this structure type is the zigzag chains of metal atoms with a short W−W and Mo−Mo distances of 2.72 Å and of 2.92 Å, respectively. This first report was finally expanded by the three-dimensional structure determination of exfoliated-restacked WS_2 (fresh samples) by using atomic pair distribution function (PDF) analysis.[18] It provided a new description of these structures which does not fit with previous models, especially those arising from EXAFS studies. EXAFS does not seem to allow an accurate estimation of the actual structure of these exfoliated materials, but it is however a short-range technique that offers an opportunity to validate the three-dimensional structure deduced from the PDF long-range analysis and to discuss the degree of reliability of structural models that were reported previously. However, whatever the conclusions, all the previous reports shared a common problem regarding the correct estimation of the number of neighbors by EXAFS for highly disordered structures: the total number of neighbors around the cation (Mo or W) is always expected to be six but an estimation of 3−4 sulfur atoms around the cation was found more frequently. This meaningless value was always assigned to a strong disorder effect but the usual approach based only on a Gaussian disorder (translated by the Debye-Waller factor) led to erroneous results, as proved not only by the wrong number of neighbors, but also by some longer metal−sulfur distance reported.[10] Therefore, it was necessary to confirm the accuracy of the structural model deduced from both electron diffraction and PDF analyses. Hence, we undertook X-ray absorption studies at the W L_{III} edge of restacked and pillared WS_2, but the analysis was performed with the introduction of a new structural parameter, the broadening *s* of a hard sphere distribution convoluted with the usual Gaussian dispersion.[19, 20]

Experimental Section

Sample Preparation. Samples were synthesized following a procedure that has been described in detail elsewhere.[3] The following compounds were studied for this work: 2H−WS_2, restacked WS_2 (res-WS_2), $[Ni_9S_9(PEt_3)_6]_xWS_2$ (**1**), $[Co_6Te_8(PBu_3)_6]_xWS_2$ (**2**), $[Fe_6S_8(PEt_3)_6]_xWS_2$ (**3**), $[Co_6Se_8(PPh_3)_6]_xWS_2$ (**4**), and $[Co_6S_8(PPh_3)_6]_xWS_2$ (**5**). Compounds were prepared about one month before the experiments and they were stored under vacuum in sealed tubes until the sample preparation.

Tungsten L_3 edge X-ray absorption spectra were recorded at LURE, on the DCI ring using 1.85 GeV positrons with an average intensity of 250 mA. They were collected in transmission mode at the W L_3 edge (calibrated on the white line at 10 204 eV), on the EXAFS 13 and EXAFS 4 spectrometers. EXAFS was recorded from 10 150 to 11 200 eV with a 2 eV step (2 s time counting) with a Si (111) double crystal monochromator. X-ray absorption near edge structure (XANES) was recorded with a three step procedure: 10 000 to 10 180 eV (3 eV step, 2 s counting); 10 180 to 10 240 eV (0.3 eV step, 2 s counting); and 10 240 to 10 400 eV (3 eV step, 2 s counting) using a Si (311) monochromator. The energy was calibrated with a tungsten foil. Three spectra were recorded for every EXAFS spectrum and their intensities were averaged before analysis. Spectra at the Sulfur K edge were recorded on the SA32 beam-line (SACO ring), with a Ge (111) double crystal monochromator, between 2450 and 2570 eV (0.2 eV step, 1 s time counting).

The EXAFS analysis was performed according to the curved-wave single scattering theory[21−23] once the absence of significant multiple scattering contributions had been checked in the studied region. The background absorption was calculated by using a theoretical expression,[24] and the single atomic absorption of the absorber was interpolated by a fifth degree polynomial, followed by (if required) smoothing. The energy of the edge *E*o was taken at the half-height of the absorption (10 197 eV). The RDF—actually a pseudo-radial distribution function because distances are not corrected from atomic potentials phase shift—was obtained by a Fourier transform of the weighted $\omega(k)\cdot k^3\cdot\chi(k)$ spectra, where $\omega(k)$ is a window using a Kaiser function ($\tau = 2.5$) defined between 2.5 and 16 $Å^{-1}$. All the further back-Fourier transforms include a removal of this window. Structural parameters were fitted by using both simplex and least-squares calculations.[25] EXAFS extraction and single scattering fit were performed with the EXAFS for Mac software [26] and multiple scattering calculations as well

(11) Lemaux, S.; Golub, A. S.; Gressier, P.; Ouvrard, G. *J. Solid State Chem.* **1999**, *47*, 336.
(12) Bissessur, R. Thesis, Michigan State University, Lansing, MI, 1994.
(13) Rocquefelte, X.; Boucher, F.; Gressier, P.; Ouvrard, G.; Blaha, P.; Schwarz, K. *Phys. Rev. B* **2000**, *62*, 2397.
(14) Heising, J.; Kanatzidis, M. G. *J. Am. Chem. Soc.* **1999**, *121*, 11720.
(15) Tsai, h.-L.; Heising, J.; Schindler, J. L.; Kannewurf, C. R.; Kanatzidis, M. G. *Chem. Mater.* **1997**, *9*, 879.
(16) Heising, J.; Kanatzidis, M. G. *J. Am. Chem. Soc.* **1999**, *121*, 638.
(17) Brown, B. E. *Acta Crystallogr.* **1966**, *20*, 268.
(18) Petkov, V.; Billinge, S. J. L.; Heising, J.; Kanatzidis, M. G. *J. Am. Chem. Soc.* **2000**, *122*, 11571.
(19) Prouzet, E.; Michalowicz, A.; Allali, N. *J. Phys. IV* **1997**, *7*, C2/261.
(20) See Supporting Information.
(21) Lytle, F. W.; Sayers, D.; Stern, E. A. *Phys. Rev. B* **1975**, *11*, 4825.
(22) Stern, E. A.; Sayers, D.; Lytle, F. W. *Phys. Rev. B* **1975**, *11*, 4836.
(23) Teo, B. K. *EXAFS: Basic Principles and Analysis*; Berlin, 1986.
(24) Lengeler, B.; Eisenberger, P. *Phys. Rev. B* **1980**, *21*, 4507.
(25) James, F.; Roos, M. CERNID internal report, 1976.

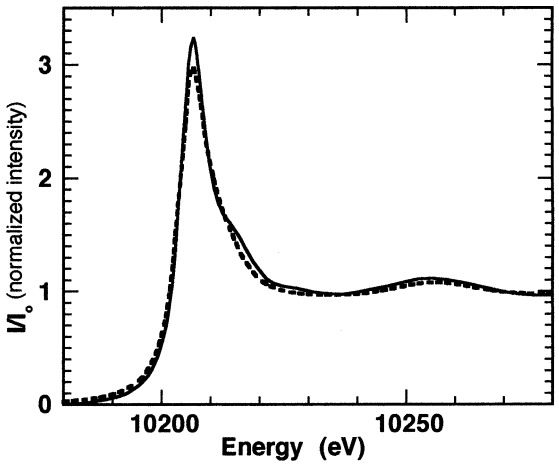

Figure 1. X-ray absorption spectrum at the W L_3 edge, for *2H*-WS_2 (line) and res-WS_2 (dashed).

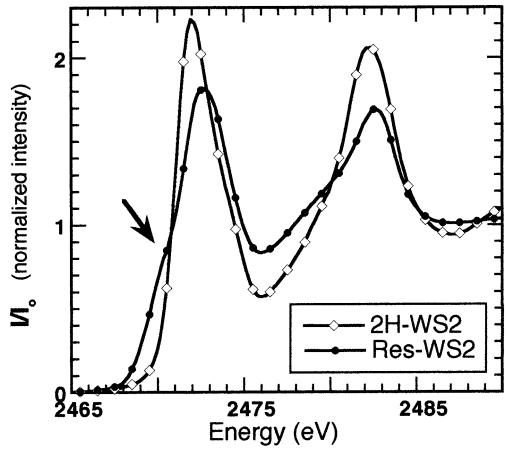

Figure 2. X-ray absorption spectrum at the S K edge, for *2H*-WS_2 (line) and res-WS_2 (dashed).

as theoretical amplitude $A(k)$ and phase shift files $\Phi(k)$ determination with the FEFF 7 Code.[27,28] The disorder was taken into account through a model based on a hard sphere distribution that introduces an additional asymmetry parameter.[19,20] The fitting procedure is thus performed according to the following EXAFS equation:[19]

$$k\cdot\chi(k) = -S_0^2\cdot\sum_i N_i A_i(k)\frac{(1+2ks_i\cdot\mathbf{cot}(2kR_i+\Phi))}{(4k^2s_i^2+1)(R_i+s_i)^2}\cdot e^{-2k^2\sigma^2}\cdot e^{2\Gamma(Ri+si)/k}\cdot\mathbf{sin}(2kR_i+\Phi) \quad (1)$$

Results

First, we compared the XANES for *2H*-WS_2 and res-WS_2. Normalized XANES spectra at the tungsten L_{III} edge and at the sulfur K edge are displayed in Figures 1 and 2, respectively. The W edge structure remains almost identical during the exfoliation/restacking procedure, which proves that no byproducts, neither metal nor oxide, form. It has been shown previously with TaS_2 that the sulfur K edge structure is very sensitive to structural changes, and that the XANES at this edge is a very good fingerprint for discriminating between

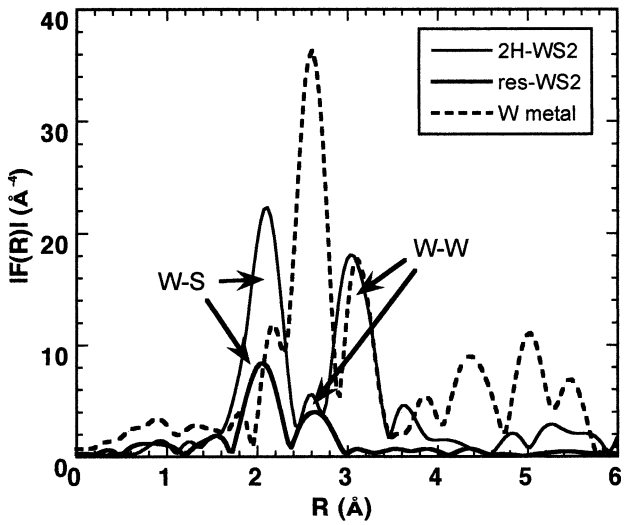

Figure 3. RDF at the W L_3 edge of *2H*-WS_2 (line), restacked WS_2 (bold line), and metal W (dashed). Except for the intensity decrease between *2H*-WS_2 and res-WS_2, the main difference is the shortening of the W−W distances (second shell).

1T- and *2H*-type structures.[29] In Figure 2, we observe a peak at ∼2483 eV, due to a small amount of S atoms in the +6 oxidation state, that is a sulfate ion SO_4^{2-}. Such a feature has been already observed in similar phases.[8] The first peak at 2472 eV presents several changes. The reduction of its intensity must be considered carefully because it is highly dependent on the sample orientation and the beam polarization.[7] For the well-crystallized *2H*-WS_2, lamellar particles tend to exhibit a preferential orientation with slabs stacked parallel to the substrate, whereas res-WS_2 will stack more randomly, which prevents any comparison between peak intensities. However, one sees the occurrence of a shoulder at lower energy (arrow), which is due to changes in the sulfur environment, but one does not see the splitting of the electronic d levels that would be expected if a pure *2H*- to the hypothetical *1T* transition were present.[11]

The modulus of the Fourier transforms (heretofore called RDF) of *2H*-WS_2, restacked-WS_2 (res-WS_2), and a tungsten foil, are displayed in Figure 3 (the distances are uncorrected from phase shift). For *2H*-WS_2, the first peak at 2.0 Å corresponds to the first sulfur shell around W and the second peak at 3.1 Å corresponds to the second shell, that is, the W atoms in the adjacent sites. As already observed,[30] there is a drastic change, especially a decreasing intensity in the RDF of restacked WS_2. The first peak (sulfur shell) appears at the same distance as that for *2H*-WS_2, but the peak at ≈3.1 Å, assigned to W in *2H*-WS_2, has vanished and a new peak appears at a shorter distance of 2.8 Å, which cannot be assigned to a minor phase such as tungsten metal. As stated above, authors agree that this peak corresponds to the second shell around the absorbing atom in res-WS_2, and not to a byproduct. This metal−metal bond shortening is in line with previous EXAFS results and our PDF analysis that pointed out a 0.08 Å shortening of the W−W distance.[18] Unlike MoS_2, restacked WS_2 is very stable, and it does not convert to the *2H* structure,

(26) Michalowicz, A. *J. Phys. IV* **1997**, *7*, c2/235.
(27) Rehr, J. J.; Mustre de Leon, J.; Zabinsky, S. I.; Albers, R. C. *J. Am. Chem. Soc.* **1988**, *110*, 3763.
(28) Mustre de Leon, J.; Rehr, J. J.; Zabinsky, S. I. *Phys. Rev. B* **1991**, *44*, 4146.
(29) Moreau, P. Nantes, France, 1994.
(30) Joensen, P.; Frindt, R. F.; Morrison, S. R. *Mater. Res. Bull.* **1986**, *21*, 457.

Table 1. Results of the Fits of the EXAFS Spectra for *2H*-WS_2, Res-WS_2, and Compounds 1−5[a]

	Gaussian model		asymmetric model						
	2H-WS_2	Res-WS_2	*2H*-WS_2	Res-WS_2	**1**	**2**	**3**	**4**	**5**
				Sulfur					
N	(6)	2.9	(6)	5.5	6.6	5.2	5.8	5.1	6.0
R (Å)	2.40	2.42	2.40	2.35	2.35	2.35	2.36	2.36	2.36
σ (Å)	0.04	0.06	0.04	0.01	0.03	0.03	0.03	0.03	0.04
s (Å)	−	−	0.0002	0.17	0.15	0.10	0.11	0.09	0.08
ΔEo (eV)	9.1	9.6	9	7.5	11.5	9.8	10.1	9.4	10.0
				Tungsten					
N	(6)	1.1	(6)	1.94	2.3	2.5	2.6	3.7	2.9
R (Å)	3.15	2.73	3.15	2.75	2.75	2.75	2.76	2.74	2.74
σ (Å)	0.05	0.06	0.05	0.075	0.07	0.07	0.07	0.08	0.07
s (Å)	−	−	0.0	0.004	0.0	0.0	0.0	0.0	0.0
ΔEo (eV)	7.6	2.7	7.6	8.9	9.2	9.0	9.1	7.0	9.4
ρ (%)	3.5	2.3	3.9	1.0	1.4	2.2	4.8	4.3	2.0

[a]For each shell, the parameters were the number of neighbors *N*, the actual distance between the absorber and the backscatterer *R*, the DW factor *σ*, and the energy shift Δ*E*o. A supplementary parameter *s* was fitted with the asymmetric model. *ρ* is the error residue calculated from eq 5.

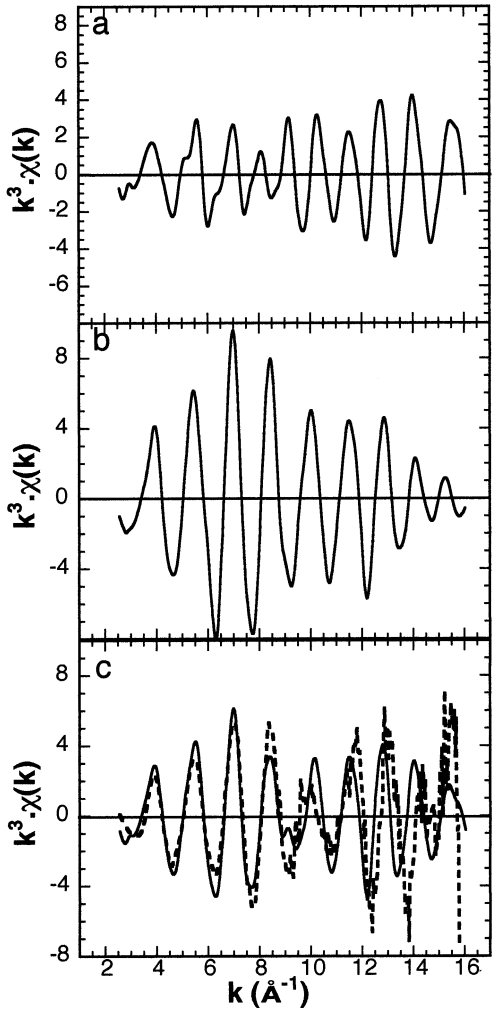

Figure 4. Comparison of the EXAFS contributions for res-WS_2 structure: (a) Feff calculation around the W1 atom; (b) Feff calculation around the W2 atom; and (c) comparison of the total Feff calculation (line) obtained by the averaging of (a) and (b) with the experimental spectrum (dashed).

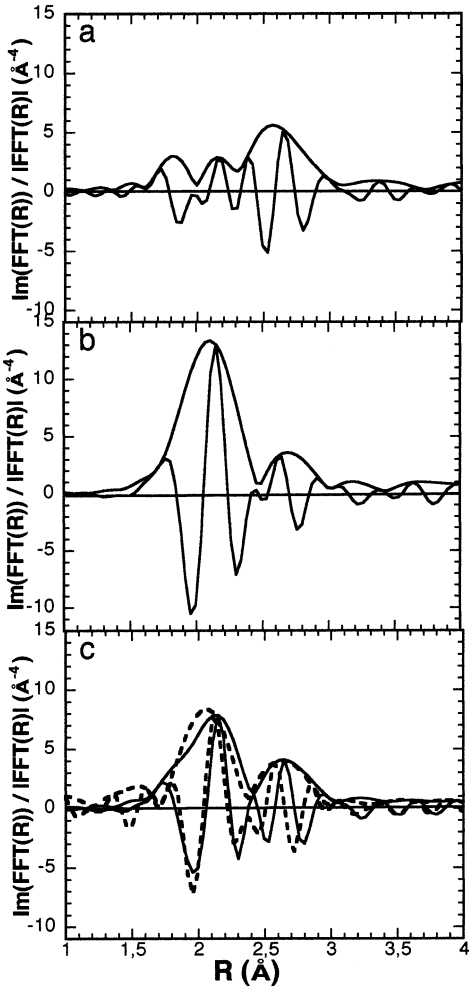

Figure 5. Comparison of the FFT imaginary part and modulus for res-WS_2 : (a) Feff calculation around the W1 atom; (b) Feff calculation around the W2 atom; and (c) comparison of the theoretical EXAFS spectrum (line) obtained by the averaging of (a) and (b) with the experimental spectrum (dashed).

even after months. At this point, one may also comment on the particular shape of the W peak, observed in the RDF of both WS_2 and W. The shoulder observed at a shorter distance from the main peak originates only from a specific shape of the atomic phase shift with the wave vector, which is not linear and leads to more complex peak shapes than usual.

We applied the two structural models—Gaussian and asymmetric—to the *2H*-WS_2 and res-WS_2 samples and compounds **1**−**5**. The asymmetric model was first tested on *2H*-WS_2 in order to confirm that a zero value is found for the *s* parameter when applied on a well-ordered material. Results are given in Table 1. First, a fit of *2H*-

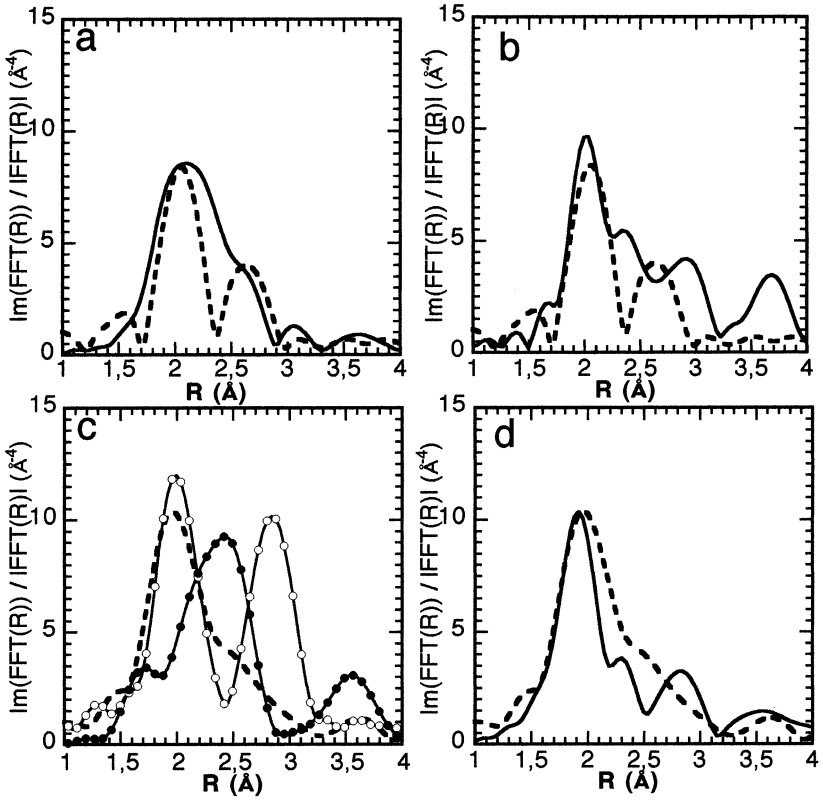

Figure 6. Comparison of the RDF for different structural models: (a) res-WS_2 (dashed, this study) versus the structure deduced from TEM microdiffraction (line);[16] (b) res-WS_2 (dashed, this study) versus the structure extrapolated from a pure WTe_2 symmetry (line); (c) res-MoS_2 (dashed, courtesy of G. Ouvrard) versus the res-Mos_2 models calculated either from the fit results (white dots) or calculated from the structural model (black dots) in ref 10; (d) res-MoS_2 (dashed, courtesy of G. Ouvrard) versus the zigzag res-Mos_2 model obtained by Rocquefelte et al. by a FPLAPW method (line).[13]

WS_2, with the number of neighbors kept constant according to the crystallographic structure,[31] allowed us to determine the Γ values for the sulfur and tungsten shells, which were 0.72 and 0.48 Å^{-2}, respectively. These parameters were kept constant for the remainder of the analysis. The double shell fit was performed once we checked that there was no significant multiple scattering contribution in the spectra. The Gaussian model applied to *2H*-WS_2 leads to W−S distances of ∼2.40 Å and W−W distances of 3.15 Å, in very good agreement with crystallographic data (2.403 and 3.153 Å, respectively).[31] Applying the asymmetric distribution model did not improve the fit reliability and it converged toward a zero value for the asymmetry parameter *s*. Unlike *2H*-WS_2, a Gaussian fit of res-WS_2 gave structurally meaningless results, especially regarding the number of neighbors in the sulfur shell. The application of the asymmetric distribution fit to the S shell leads to a very good agreement between experimental data and model.[20] Thus, the asymmetric model allowed us to find the expected value for the sulfur neighbors, (i.e., a value close to 6), as well as a shortening of the W−S distance, compared with previous results. These results show that the Gaussian model applied to this disordered shell led, as expected, to an underestimation of the number of neighbors and an overestimation of the actual distances.

Quite surprisingly, the sulfur shell is highly asymmetric ($0.08 \leq s \leq 0.17$) but the tungsten shell remains quite ordered ($\sigma = 0.075$ Å, $s = 0.004$). Therefore, the low number of W neighbors—the apparent mean number of W neighbors is thus of 2.7 when averaged among all samples—cannot be ascribed to a wrong determination but to an actual decrease of the neighbors of tungsten probed by the absorbing atom. The lack of signals from the other backscattering W atoms does not mean that they disappeared but that their respective positions have been distributed in such a way that gave rise to destructive interferences between their backscattering. In addition, one may notice that intercalation of clusters (samples **1**−**5**) does not modify the structure of the restacked WS_2, compared with the nonintercalated res-WS_2. The *s* values, between 0.08 and 0.17, correspond to a broad distribution of the W−S distances in the WS_6 site. Moreover, one observes a shrinking of the W−W distance, from 3.15 Å in *2H*-WS_2 to 2.75 Å for res-WS_2. The shortening of W−W distances, the broad distribution of W−S distances, and the apparent reduction of W neighbors from 6 to 2−3, can be explained by only a shift of the W atom from its ideal position in pristine *2H*-WS_2 toward a new position, which agrees with a "clusterization" of the W atoms forming the zigzag chains. Such a shift would explain the broad distribution of the W−S distances, which cannot be fitted by a simple Gaussian model.

Even if EXAFS by itself cannot solve the structure, it is a perfect local probe to validate different structural models that may represent an averaging between several local structures. Hence, the EXAFS analysis, along with theoretical calculations of the EXAFS spec-

(31) Schuttle, W. J.; de Boer, J. H.; Jellinek, F. J. *J. Solid State Chem.* **1987**, *70*, 207.

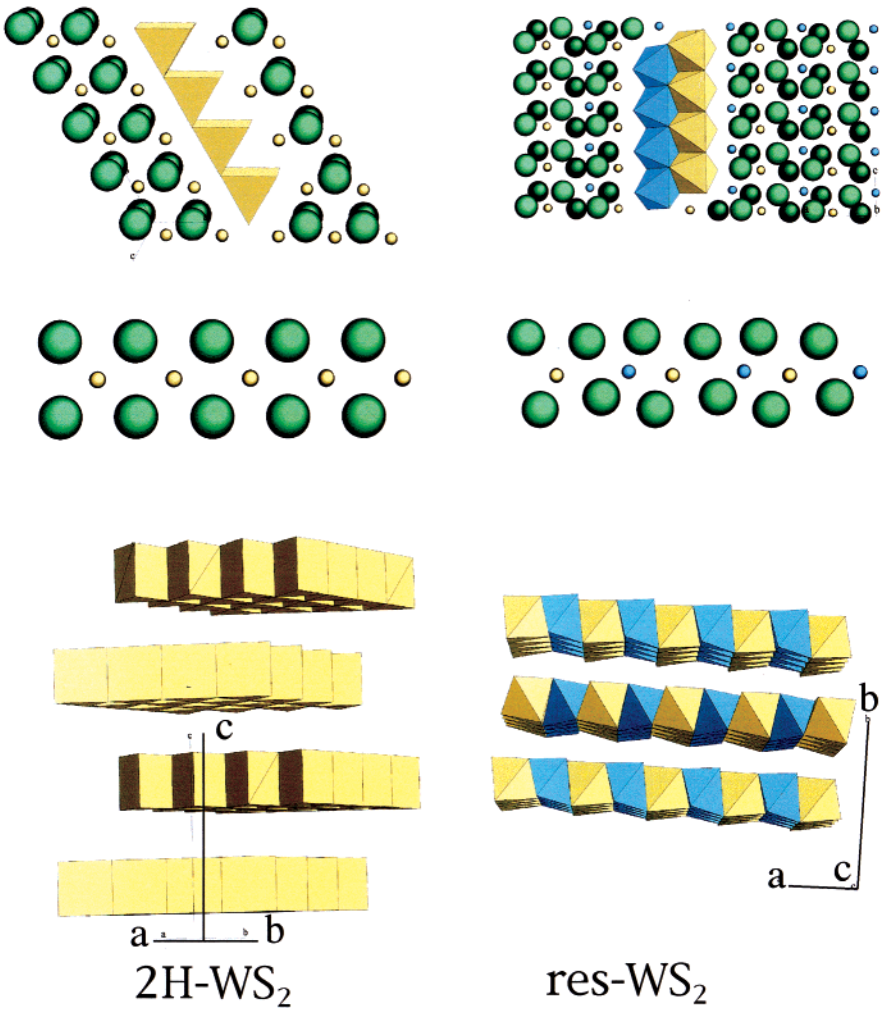

Figure 7. Comparison between the *2H*-WS_2 structure (left) and the res-WS_2 one (right)

trum expected from structural models, including PDF results, should provide a full understanding of the effective structure of res-WS_2. The calculation was performed with FEFF 7.0 Code in a 10-Å radius sphere around the absorbing atom taken at central atom, and scattering paths from 2 to 6 legs were taken into account. This approach was first tested on crystalline *2H*-WS_2, with crystallographic data ($P6_3/mmc$ space group, $a = b = 3.153$ Å, $c = 12.323$ Å, W (0.3333, 0.6667, 0.25), S (0.3333, 0.6667, 0.6225)) with a very good agreement between theoretical and experimental spectra.[20,31] This approach was then applied to test structural models for unknown structures.

Computing of the structure of res-WS_2 deduced from the PDF analysis was performed from the atomic positions calculated by Petkov et al.[18,20] Because tungsten can be in two crystallographic positions, the simulation was performed for each of the two different W atoms, then the results were averaged. For the calculation, 170 and 179 scattering paths were retained for the W1 and W2 atoms, respectively, and their respective DW contributions were qualitatively estimated.[20] EXAFS contributions were further averaged, as well as the real and imaginary parts of the FFT.[20] Figure 4 displays the EXAFS contribution of each W atom, along with the comparison of the total EXAFS spectrum with the experimental one. Figure 5 displayed the relative imaginary part and modulus of these contributions. It appears that the environment around W1 is much more distorted than the one around W2, which leads to a strong decrease in intensity for the W1 contribution. The agreement with the experimental data is still rather good, which confirms that the structure deduced from PDF is essentially correct.

Discussion

Since their first report, both WS_2 and MoS_2 exfoliated materials have been extensively studied and several structural models were proposed. However, until now, none were compared with experimental observations. Therefore, we carefully compared the calculated EXAFS spectra from these models with the actual EXAFS spectra of both restacked WS_2 or MoS_2, to check whether any of them could also describe the experimental results. Results are displayed in Figure 6 (intensities were roughly adjusted). Figure 6a describes the comparison between the 2D-model proposed by Heising and Kanatzidis, deduced from micro-diffraction TEM analysis, where they proposed that the res-WS_2 possessed zigzag metal chains.[16] The agreement is rather good. In Figure 6b, the comparison of this structure with a pure WTe_2-type structure extrapolated from the crystalline data of WTe_2 is not straightforward. Figure 6c displays the comparison of res-MoS_2 with two structural models proposed by Dungey et al.[10] The first one (white dots) is calculated from the fitting results provided in

their publication whereas the second one (black dots) is calculated from the crystallographic structure proposed in the same report. It is obvious that these hypotheses do not fit with the experimental data obtained on freshly restacked MoS_2. It is also puzzling that the direct fitting of their own data and the crystallographic model do not agree. Finally, we report in Figure 6d the comparison of a last structural model extrapolated from FPLAPW calculations by Rocquefelte et al. on $LiMoS_2$.[13] In that case, the agreement with the actual RDF is good. The structure of $LiMoS_2$ has been recently experimentally determined for the first time. The approach of atomic pair distribution function (PDF) analysis was used because of the lack of well-defined Bragg peaks due to the short structural coherence (∼ 50 Å) in this intercalation compound. The PDF analysis confirms the Rocquefelte et al model and shows clearly that the reduction of Mo by Li leads to similar phenomena with the formation of Mo−Mo bonding and the formation of diamond-like chains of distorted $Mo-S_6$ octahedra.[32]

(32) Petkov, V.; Billinge, S. J. L.; Larson, P.; Mahanti, S. D.; Vogt, T.; Rangan, K. K.; Kanatzidis, M. G. *Phys. Rev. B* **2002**, *65*.

The EXAFS analysis results reported here fully support the conclusions of the PDF analysis and 2D electron crystallographic determination. A full description of the restacked WS_2 phase may thus be drawn and compared with the pristine *2H*-WS_2 (Figure 7). *2H*-WS_2 exhibits a perfect undistorted structure with all W atoms in trigonal prismatic sites and all S atoms equivalent. The res-WS_2 structure presents two types of distorted octahedral sites for the two nonequivalent W atoms. These octahedra are linked together to build the zigzag chain previously proposed. These sites are too distorted and cannot be described by a hypothetical *1T* structure. Moreover, the local shift of the W atoms is in tandem with a periodic shift of the S atoms along the stacking axis (*b* axis for our calculation), that causes the layer to deviate from full planarity.

Acknowledgment. Support of this research by NSF-CRG grant CHE 99-03706 is gratefully acknowledged.

Supporting Information Available: Comparisons of EXAFS and Fourier transform spectra, scattering paths and atomic postions for the subject compounds, and EXAFS analysis discussion (PDF). This material is available free of charge via the Internet at http://pubs.acs.org.

CM021186Z